Two-phase jet dispersion

P. Bricard, L. Friedel *

Technische Universität, Hamburg-Harburg, AB Strömungsmechanik, D-21071 Hamburg, Germany

Abstract

This paper presents the state-of-the-art in the field of hazardous dispersion with special attention to two-phase jet conditions. After recalling the specificity of two-phase jet dispersion, the uncertain features of the integral and multidimensional models are discussed and specific suggestions for improvement are proposed. The boundary conditions corresponding to the rapid flow change just downstream of the orifice due to flashing, gas expansion and droplet formation are also considered. The lack of adequate two-phase jet dispersion data and the resulting poor validation of the models are particularly pointed out. © 1998 Elsevier Science B.V.

Keywords: Two-phase flow; Jet; Dispersion; Modelling; Review

1. Introduction

After the extremely serious accidents which happened in the chemical, petrochemical and petroleum industry in the last 3 decades, the safety authorities have to reconsider the procedures and the models dedicated to the assessment of potential hazards. In particular, one may have to determine the impact on the environment of an accidental release of

---

Abbreviations: A, Cloud cross-section area; c, Concentration; C, Cloud cross-section perimeter; C_D, Drag coefficient; d, Drop diameter; D, Cloud cross-section diameter; E, Entrainment function; F, Force; F_D, Drag force; g, Acceleration of gravity; h, Specific enthalpy; Re, Reynolds number; Ri, Richardson number; s, Curvilinear coordinate; u, Velocity; u', Turbulent intensity; u_*, Friction velocity; We, Weber number; x, y, z, Cartesian coordinates; *Greek symbols:* α, Empirical constant; ΔU, Relative velocity; ρ, Density; σ, Surface tension; σ_y, σ_z, Pasquill–Gifford dispersion coefficients; θ, Angle between cloud axis and horizontal; *Subscripts:* a, Ambient air; c, Centreline; g, Gas; m, Average over the jet cross-section; max, Maximum stable; p, Particle; x, x-direction; z, z-direction; 0, Outlet; 1, Related to jet turbulence; 2, Related to cross-flow; 3, Related to atmospheric turbulence

* Corresponding author.

toxic or flammable chemicals. Many releases to be considered involve high-momentum two-phase discharges. This may occur from emergency venting of vessels due to fire exposure or runaway reaction, or from accidental breaches in vessels, pipes or sealings. In the case of storage of pressurized liquefied gas, venting induces flashing of the superheated liquid; in the case of thermal runaway reactions, gassy reaction products can be released with the liquid phase. Releases involving two-phase flow exhibit specific characteristics which can significantly influence the dispersion process. The rather recent realization of the importance of these effects has led to the development of two-phase dispersion models. A comparative review of these models is proposed here. To clarify the situation under study and to introduce basic definitions, a description of the phenomena taking place in the dispersion process is first recalled.

2. Dispersion process

Although some of the considered models may also handle other situations, we focus here on high-momentum atmospheric releases of a liquefied gas or two-phase fluids through a break or a pressure relief system. The release is supposed to originate from a relatively small hole so that continuous, i.e. quasi-steady, conditions at the outlet can be assumed. The *cloud* is defined as the smallest control volume containing the contaminant. In its first stage, where its initial momentum dominates, the cloud will also be referred to as *jet*. In most cases involving two-phase releases, the flow is choked at the exit and an external depressurization zone, where the pressure decreases down to the atmospheric pressure, is formed. When the exiting liquid is sufficiently superheated with respect to ambient conditions, it is atomized by violent vaporization (flashing atomization). Otherwise, the liquid or two-phase mixture is disintegrated due to liquid surface instabilities (aerodynamic atomization). Downstream from this region, air entrainment at the perimeter of the cloud becomes important, which causes it to further widen. At least for some distance, the cloud may be dense, i.e. heavier than air, as a result of high molecular weight (e.g. chlorine) or low temperature and airborne droplets (e.g. evaporating ammonia) [1].

The dispersion of the contaminant in the atmosphere can be described in terms of cloud *trajectory* and *dilution*. From an integral point of view, the *trajectory* is given by a momentum balance on the cloud; the main effects involved are cross-wind, gravity and friction on the ground after touchdown. The *dilution* is controlled by the rate of air entrained in the cloud. Near the outlet, this is governed by the turbulence generated by the jet itself; it is then controlled by atmospheric turbulence when the jet velocity has decreased close to that of the ambient wind. Moreover, the interaction with a cross-wind induces an enhancement of the entrainment rate. In the case of dense clouds, gravity may also have an effect on air entrainment, related to gravity-induced turbulence as well as suppression of atmospheric turbulence due to stable stratification. In the following, the region of passive dispersion due to atmospheric turbulence only is referred to as the *far-field* and the upstream region as the *near-field*.

The dispersion process may be significantly affected by the presence of an aerosol phase. First, two-phase releases can lead to much higher discharge mass flow rates than

single-phase gas releases [2] and, thus, increase the hazard zone distance. Moreover, the jet density may be significantly higher. It can firstly be increased by the mere presence of the liquid phase. However, this is only significant very close to the outlet, where the liquid mass fraction averaged over the jet cross-section is not negligibly small. The aerosol effect on jet density is mainly due to phase change phenomena. When the liquid contaminant evaporates, the jet may significantly cool down and, thus, increase in density. A gas which has a smaller molecular weight than air like ammonia can then behave as a heavy gas. The cooling process may also lead to the condensation of the entrained humidity. If the contaminant is hygroscopic, this can lead to its persistence to significantly larger distances from the outlet. The formation of the aqueous aerosol will cause the mixture to warm up more rapidly and have less density [3]. Furthermore, a part of the liquid may not remain airborne in the jet and fall to the ground where an evaporating pool could build up; such a pool may also be formed from the jet impingement on a surface. This so-called *rainout* could induce a drastic reduction of the downstream contaminant concentration but increases the danger close to the source as well as the duration of the dispersion. Besides, it may lead to soil contamination. Finally, the presence of the aerosol also affects the turbulent structure of the jet and, therefore, the air entrainment, the direction of influence (enhancement or suppression) depending on the particle size.

3. Two-phase dispersion models

The dispersion models which take into account the presence of an aerosol phase have appeared only recently (in the last decade) in the literature. They are either integral or multidimensional models. Integral models are obtained by integrating the balance equations for mass, momentum, energy and species over the cloud cross-section. The lateral variations of the local variables, such as velocity, concentration and temperature, can be obtained by introducing lateral profiles in the integrated balance equations. If these profiles are flat ('top-hat' profiles), the model reduces to the so-called 'box' model. Nonuniform profiles, which are supposed to be geometrically similar after a zone of flow establishment, can also be adopted. In multidimensional models, the local time-averaged equations of mass, momentum, energy and species are locally solved in the whole space. Unlike the integral models where turbulent diffusion is implicitly given through the profile shape function, closure must be provided for turbulent stresses.

Because of the high variety of possible situations to be considered in hazard assessment, but which cannot or have not been covered by experiments, the dispersion models are often extrapolated beyond the range where they have been validated. The need for physically-based models is, therefore, very important to increase the reliability of this extrapolation. Moreover, due to the frequent need to study a large number of scenarios, a compromise between model detail and computing time/cost is often required. These conditions are best fulfilled by one-dimensional (integral or box) models, which can be in most cases helpful. However, in some situations associated with obstructed terrain, multidimensional models could be recommended, as it is shown, e.g., by Würtz et al. [4]. They are however complex, costly to run and often faced with numerical difficulties, and require a high degree of expertise.

In the following description, every necessary jet property at the outlet, such as the mass flow rate, is supposed to be known. However, within a short distance just downstream from the outlet, the flow can experience drastic changes which must be considered for subsequent dispersion calculations. The physical phenomena taking place in this region comprise (i) flashing if the liquid is sufficiently superheated, (ii) gas expansion when the flow is choked and (iii) liquid fragmentation. The corresponding quantities to be determined as initial conditions for subsequent dispersion are the flash fraction, the jet mean temperature, velocity and diameter, and the drop size. Due to its relatively short length, a global and simplified modelling approach is normally adopted in this region, also in the case of multidimensional models. Therefore, these initial conditions are first described, followed by the description of the integral and multidimensional dispersion models.

3.1. Initial conditions

3.1.1. Flashing

Flashing occurs when the liquid is sufficiently superheated at the outlet (with respect to atmospheric conditions) and corresponds to the violent boiling of the jet. The vapour quality after flashing, or flash fraction, is most often determined in the models by assuming isenthalpic depressurization of the mixture between the outlet and the plane downstream over which thermodynamic equilibrium at ambient pressure is attained, i.e., any transfer with the surroundings as well as the kinetic energy change are neglected; the temperature reached is the saturation temperature at atmospheric conditions. It should be noted that this calculation is applied in the models as soon as the liquid is superheated.

In this approach, the neglect of the kinetic energy change seems to be justified due to the large contribution of the heat of vaporization in the energy equation [3]. However, a more general expression, where this assumption is relaxed, is recommended by Britter [5,6]. Adiabatic and frictionless conditions as well as the absence of air entrainment are reasonable approximations provided that the distance up to the point where thermodynamic equilibrium at atmospheric pressure is reached, is short enough. Atmospheric pressure is in general attained after a flow length of about two orifice diameters and the flashing phenomenon is observed to occur very fast so that these assumptions should be met in practice. When the liquid is not sufficiently superheated for flashing atomization to occur, the flow path before thermodynamic equilibrium is restored, could be greater. However, the degree of non-equilibrium being low in this case, the above assumptions should still be acceptable.

3.1.2. Expansion

When the flow is choked at the outlet, the gas phase expands to ambient pressure within a downstream distance of about two orifice diameters. This causes a strong acceleration of the two-phase mixture and usually an increase of the jet diameter. In the models, the velocity and diameter of the jet at the end of the expansion zone are given by the momentum and mass balance, respectively, integrated over a control volume extending from the outlet to the plane where atmospheric pressure is first reached. It is

assumed that no air is entrained in this region. An alternative model based on isentropic expansion has been proposed by Woodward [7]. This led to substantially different results.

This control volume approach, which cannot provide the variations within the expansion zone, appears to be suitable in view of its short length. The absence of air entrainment is also justified by the strong lateral expansion. Because of the lack of experimental data, the alternative predictions obtained by using the model of Woodward could not yet be validated. Finally, it should be noted that the flow speed can be increased by a factor as high as 10 in this region, which has important consequences on the downstream dispersion [3].

3.1.3. Drop size

The models incorporating fluiddynamic and thermodynamic non-equilibrium phenomena, like rainout or droplet evaporation, require submodels for the determination of the initial drop size. There are basically two main mechanisms for atomization: flashing and aerodynamic atomization. With flashing atomization, the fragmentation results from the violent boiling and bursting of bubbles in the superheated liquid, whereas aerodynamic atomization is the result of instabilities at the liquid surface. Most authors do not use any specific criterion to determine which mechanism dominates and deliberately select one of them. Nevertheless, Ianello et al. [8] use a mechanistic criterion based on a critical superheat corresponding to the activation of a nucleation site. It requires, however, the specification of a characteristic nucleation site radius for which reliable predictive relations are not available. Woodward and Papadourakis [9,10] consider that the actual regime is the one which predicts the smallest maximum stable drop size. A comparison of these criteria with available empirical relations relying on experiments with low velocity jets [11–13] could be fruitful. In any case, more studies on this transition region where both fragmentation regimes may play a role are clearly needed.

In the case of aerodynamic fragmentation, the maximum stable drop size is usually given by a critical Weber number, which represents the ratio of inertia over surface tension forces:

$$\mathrm{We}_{\mathrm{max}} = \Delta U^2 \rho_{\mathrm{g}} d_{\mathrm{max}} / \sigma, \tag{1}$$

where σ is the (static) surface tension of the liquid, ρ_{g} the gas density, d_{max} the maximum stable droplet diameter and ΔU the mean relative velocity between both phases. In the models, ΔU is calculated as the jet mean absolute velocity at the end of the expansion zone in the case of choked flow conditions and the subcritical outlet velocity otherwise. This implies that interfacial stress occurs at contact with the surrounding still air, which is justified in the case of a single-phase liquid jet. However, if a two-phase choked flow were to occur at the outlet, the fragmentation will be induced by the shear stress between the liquid and the accelerating released gas and, thus, a more appropriate relative velocity should be based on the difference between the jet velocity at the end of the expansion zone (representative of the gas velocity) and the exit velocity (representative of the liquid velocity).

Moreover, the number $\mathrm{We}_{\mathrm{max}}$ is taken equal to 12, 20 and 25 by Ianello et al. [8], Wheatley [14] and Woodward et al. [15], respectively. Default values ranging between

17 and 44, with a possible dependence on stagnation pressure (or exit velocity), have been tested by Muralidhar et al. [16]; their best prediction for the liquid capture on the ground was obtained with the value of We_{max} depending on pressure. According to Kolev [17], the experimental observations provide maximum Weber values between 5 and 20 for low-viscosity liquids, with the most commonly used value being 12. Ianello et al. adopt this value but considered the corresponding droplet diameter as the mean value and not the maximum stable one. The value of 20 adopted by Wheatley can be deduced from a balance on the drop between drag and surface tension forces with a drag coefficient of 0.4 [17], which is an acceptable approximation for a rigid sphere [18] in the turbulent regime ($Re_p = \Delta U d_{max}/\mu_g$ between 500 and 2×10^5) as long as the relative velocity is small enough compared to the speed of sound. This is, according to Kolev [17], an upper limit for the maximum stable droplet diameter d_{max} since in reality the particle is deformed and experiences a higher drag during the fragmentation process. The value of 25 is proposed by Woodward and Papadourakis by reference to the work of Brown and York [11]. However, this value was actually not proposed by Brown and York for the drop size but for the jet to distinguish between two regions for the necessary superheat for flashing; it is therefore, not justified here. In Muralidhar et al.'s model the relatively high values of We_{max} as well as its dependence on the exit velocity may be due to incompleteness in other parts of the global model. In any case, the need for checking these criteria against drop size data is evident. Although obtained for relatively small orifices (≈ 1 mm) and high pressures (> 50 bar), correlations devised for the analysis of diesel-type injectors [19] could serve this purpose. In particular, the correlation proposed by Elkotb [20] shows a dependence on the reciprocal value of the exit velocity in agreement with a modified Weber number formula used by Muralidhar et al. Besides, it should be noted that the drop size predicted by Rayleigh's formula in the case of very low jet speed is additionally used in some of the above models; it does not apply, however, to the high initial momentum jet conditions we consider in this study.

For the flashing atomization, Ianello et al. [8] propose a mechanistic model based on a Weber number where the characteristic relative velocity ΔU is composed of two components, in the axial and radial direction, respectively. The axial component is due to the vapour acceleration in the expansion zone; the relative velocity is taken as the difference between the jet velocities at the end and at the beginning of this zone. The radial component comes from the momentum transfer caused by the rapidly growing bubbles; it is given by the maximum bubble expansion velocity as deduced from Forster and Zuber [21]. On the other hand, Woodward and Papadourakis [10] have established a correlation for the maximum stable diameter to match rainout experimental data. As indicated by the authors, this relation may not necessarily agree with values measured independently because of incompleteness in some other parts of the dispersion model. Among the relations they considered, the one depending on a so-called 'partial expansion energy', which is a measure of the superheat, gave the best results. Moreover, some authors adopt constant default values for the drop size based on experimental results. They usually range between 10 and 100 μm [22–24]. The predictions of the above proposed expressions should be checked against drop size data in flashing flow. The data recently obtained by Hervieu and Veneau [25] for flashing propane could

contribute to the validation of these submodels. Moreover, it should be noted that if flashing occurs upstream from the orifice (e.g. in a long pipe), the different flow regimes at the exit could lead to specific fragmentation processes, as shown by the drop size data obtained for the aerodynamic fragmentation of a dispersed-annular flow regime by Lemonnier and Camelo-Cavalcanti [26].

Regarding the assumed drop size distribution, every model considers a unique equivalent size except Ianello et al. [8] who adopt a log-normal distribution and Pereira and Chen [24] who use two size classes. The assumption of one-size droplets is obviously contrary to observations but simplifies the matter. A sensitivity analysis regarding this assumption should, however, be performed. The log-normal distribution proposed by Ianello et al. is based on the results of Bettis et al. [27] for instantaneous flashing releases. The root-normal distribution recommended by Faeth et al. [28] for aerodynamic atomization should also be considered.

Finally, Kukkonen et al. [29] and Nikmo et al. [30] have shown that, due to compensating effects, the droplet evaporation rate does not strongly depend on the initial drop size below 100 μm. This has been confirmed by the sensitivity analysis performed by Pattison et al. [22] with their model. On the other hand, the results of Muralidhar et al.'s model [16] show that the rainout fraction is very sensitive to the initial drop size.

3.2. Integral models

Integral models can either deal with both the near-field and far-field or consider the near-field only. In the latter case, they are regarded as source term for a far-field dispersion model. However, they are similar in principle and are, therefore, described together in the following. The dispersion models including two-phase flow that we have considered are the ones of Wheatley [14], Ianello et al. [8], Epstein et al. [31], Woodward et al. [9,15], Tickle et al. [32,33], Morud and Selmer-Olsen [34], Muralidhar et al. [16], Pattison et al. [22,35]. The situations which each model can handle are summarized in Table 1. It should be noted that these application limits are most often rather easy to extend and reflect more the stage of development of the model or its specific goals rather than inherent limitations. Some of these models can handle ground-level clouds, i.e., clouds in contact with the ground. In the following, the special features corresponding to this case are ignored and the review is restricted to elevated jets.

The models are all based on the balance equations for mass, momentum, energy and species, integrated over the jet cross-section; they mainly differ by the adopted closure relations. A common frame based on the mixture balance equations is first proposed to enable a comparison between the models. Then, the closure relations, or submodels, are described.

3.2.1. Balance equations

In the following, we assume that the cloud (or jet) centreline remains in the wind–gravity plane. Let s be the curvilinear coordinate of the cloud centreline, (x, y, z) its cartesian coordinates such that wind and gravity are oriented along the x and z

Table 1
Characteristics of the two-phase dispersion models

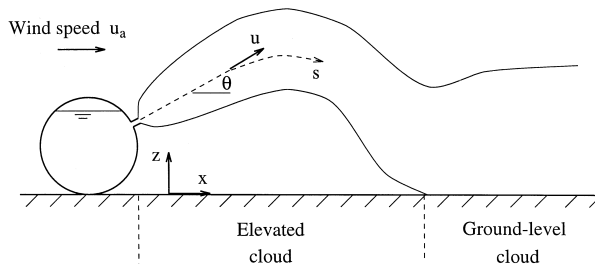| Model	Fluids	Continuous release	Instantaneous release	Cross-flow	Elevated jet	Ground-level cloud	Initial momentum	Dense cloud	Atmospheric dispersion
Wheatley	NH_3	+	−	−	+	−	+	−	−
Ianello et al.	Liquefied gas	+	−	−	+	−	+	−	−
Epstein et al.	Liquefied gas	+	−	−	+	+	+	+	+
Woodward et al.	Liquefied gas	+	+	+	+	+	+	+	+
Tickle et al.	Liquefied gas	+	−	+	+	−	+	+	+
Morud and Selmer-Olsen	Propane + inert gas	+	−	+	+	+	+	+	+
Muralidhar et al.	HF + additives	+	−	+	+	−	+	+	+
Pattison et al.	Liquefied gas	+	+	+	+	+	+	+	+

Fig. 1. Characteristics of a cloud dispersion (adapted from Ref. [31]).

directions, respectively (Fig. 1), and θ the angle between the jet centreline and the horizontal axis such that:

$$\mathrm{d}x/\mathrm{d}s = \cos\theta; \qquad \mathrm{d}z/\mathrm{d}s = \sin\theta. \tag{2}$$

With A being the cloud cross-section area, ρ, u and h, the mixture density, velocity and specific enthalpy, respectively, and c the contaminant mass concentration (in $\mathrm{kg/m^3}$) in the cloud, the balance equations for continuous (steady-state) release can then be written as:

$$\text{Mixture mass balance:} \quad \frac{\mathrm{d}}{\mathrm{d}s}\int_A \rho u\, \mathrm{d}A = E, \tag{3}$$

$$\text{Contaminant mass balance:} \quad \frac{\mathrm{d}}{\mathrm{d}s}\int_A cu\, \mathrm{d}A = 0, \tag{4}$$

$$\text{Mixture enthalpy balance:} \quad \frac{\mathrm{d}}{\mathrm{d}s}\int_A \rho uh\, \mathrm{d}A = Eh_a, \tag{5}$$

$$\text{Mixture } x-\text{momentum balance:} \quad \frac{\mathrm{d}}{\mathrm{d}s}\int_A \rho u^2\cos\theta\, \mathrm{d}A = Eu_a + F_x, \tag{6}$$

$$\text{Mixture } z-\text{momentum balance:} \quad \frac{\mathrm{d}}{\mathrm{d}s}\int_A \rho u^2\sin\theta\, \mathrm{d}A = F_z, \tag{7}$$

where E is the so-called entrainment function representing the rate of air entering the cloud; u_a and h_a are the velocity and the specific enthalpy of the ambient air, respectively; F_x and F_z are the forces which act on the jet in the horizontal and vertical direction, respectively. For ground-level clouds, additional transfer terms with the ground could be introduced in Eqs. (5) and (6). It should be noted that Ianello et al. use rather a control volume approach by integrating these equations between the origin and the current position of the jet; the closure relations do not, however, basically differ. Moreover, Pattison et al. additionally consider a momentum balance equation in the y direction to describe releases which are not in the wind/gravity plane. Furthermore, to take into account thermodynamic non-equilibrium effects, the enthalpy balance equation is separately written for the liquid and gas phase by Woodward et al., Muralidhar et al. and Pattison et al.; interfacial mass and heat transfer terms are then introduced. Finally,

Woodward et al. apply the momentum balance equation in the z-direction separately for the gas and liquid phase, adding an interfacial drag force.

3.2.2. Profiles

In the integral approach, radial profiles for velocity, density, concentration and enthalpy are introduced in the above balance equations. These profiles are supposed to be self-similar, i.e., when adequately normalized, they are expressed by a unique shape function. This allows the integrals to be replaced by mean or centreline values. A system of ordinary differential equations is then solved for u, c, A, θ, h, x, z (centreline or mean value when appropriate) provided that closure relations are given. Most models adopt the simplest possible profile, i.e. flat (or top-hat) profiles [8,14,16,31,32]. In this case, the mean and centreline values are equal and the variables are discontinuous at the cloud boundary. The form of the cross-section is supposed to be circular. More sophisticated profiles based on the Gaussian function are adopted by Woodward et al. for velocity and concentration and by Morud and Selmer-Olsen for all variables. Moreover, a different diffusion rate is considered for the velocity compared to that of the other variables via a coefficient related to the Schmidt number. Provision is also made for different diffusion rates between the vertical (z) and lateral (y) directions to take into account gravity effects. This induces an elliptic cloud cross-section.

The use of top-hat profiles gives a simple and more readable set of equations. Moreover, if needed, profiles may be 'hung' on the calculated mean values [36]. Yet, the use of Gaussian profiles is more realistic. However, in the case of vertical gas jets at different source temperature and associated with rather low exit velocities, Davidson [37] has shown that the differences between top-hat and Gaussian profiles have no significant effect on the prediction of the cloud trajectory, temperature and concentration. The validity of this conclusion should be checked for high-momentum releases. Moreover, the similarity assumption has been shown to be well verified in the case of a single-phase jet in still ambient environment after a zone of flow establishment. Popper et al. [38] observed that it was still valid for two-phase jets associated with particles smaller than 50 μm. This was further confirmed by Seifert et al. [39]. However, Moodie and Ewan [40] found that, in the case of a Refrigerant R-11 flashing jet, the similarity of the velocity profile was not achieved within a distance of 60 diameters from the exit, which is three to four times longer than in the case of single-phase gas jets. This suggests that it may be important to model this zone in more detail. This is possible, e.g. with the generalized shape function adopted by Woodward and Papadourakis [9], which allows a smooth transition in the zone of flow establishment from sharp-edge toward Gaussian profiles. Moreover, Tickle and Webber [41] mentioned that the similarity assumption is expected to fail for jets in co-flow or cross-flow when neither the jet nor the cross-flow speeds are negligible. However, according to these authors, no better practical approaches have been proposed yet.

3.2.3. Entrainment

The entrainment function E is an important item in the integral models because it controls the rate of dilution of the contaminant. This function is usually composed of several terms corresponding to different mechanisms; they are listed with a common

Table 2
Entrainment functions in the jet dispersion models

Model	Entrainment function			
	E_1	E_2	E_3	E
Wheatley	$0.08\rho_a C u_m$	–	–	E_1
Ianello et al.	$0.08(\rho_m/\rho_a)^{1/2}\rho_a C u_m$	–	–	E_1
Epstein et al.	$0.1(\rho_m/\rho_a)^{1/2}\rho_a C$ $\|u_m - u_a\cos\theta\|$	$0.5(\rho/\rho_a)^{1/2}\rho_a C u_a\|\sin\theta\|$	$\pi\rho_a u_a$ $\dfrac{d}{dx}(\sigma_y\sigma_z)$	$\max(E_1 + E_2, E_3)$
Woodward et al.[a]	$0.04(\rho_m/\rho_a)^{1/2}\rho_a C$ $(u_m\|u_c - u_a\cos\theta\|)^{1/2}$	$0.29\rho_a C u_a\|\sin\theta\|$	$5.6\pi\rho_a u_a$ $\dfrac{d}{dx}(\sigma_y\sigma_z)$	$\max(E_1 + E_2, E_3)$
Tickle et al.	$0.08\rho_a C\|u_m - u_a\cos\theta\|$	$0.6\rho_a C u_a\|\sin\theta\|$	$\alpha_3\pi\rho_a u_a$ $\dfrac{d}{dx}(\sigma_y\sigma_z)$	$E_1 + E_2 + E_3$
Morud and Selmer-Olsen	$0.028\rho_a C u_c$	$0.37\rho_a C u_a\|\sin\theta\|$	$4.6\pi\rho_a u_a$ $\dfrac{d}{dx}(\sigma_y\sigma_z)$	$E_1 + E_2\cos\theta + E_3\cos\theta$
Muralidhar et al.[b]	$0.0806(\rho_m/\rho_a)^{1/2}\rho_a C\|u_m - u_a\cos\theta\|$	$0.5\rho_a C u_a\|\sin\theta\|$	$\rho_a C u'$	$E_1 + E_2\cos\theta + E_3$
Pattison et al.[c]	$0.1(\rho_c/\rho_a)^{1/2}\rho_a C\|u_c - u_a\cos\theta\|$	$0.5\rho_a C u_a\|\sin\theta\|$	$0.28\rho_a C u_*$	$E_1 + E_2\cos\theta + E_3$

[a]E_1 is deduced from Ref. [9] with $m_{cld} = \rho_m\,u_m C^2/4\pi$.
[b]See Ref. [16] for the relations for u' in E_3.
[c]The original formula are reported here assuming the cloud axis in the wind–gravity plane; see Ref. [22] for the relations for u_* in E_3.

notation in Table 2. The contribution due to the jet turbulence is modelled as an extension to cross-wind conditions (when cross-flow is considered) of two well-known entrainment formulas for jets into still environment. The first one was proposed by Morton et al. [42]:

$$E_1 = \alpha_1 \rho_a C u, \tag{8}$$

where θ_a is the density of the ambient air, C the cross-section perimeter and α_1 an empirical constant. The velocity u can either be the centreline velocity u_c or the mean jet velocity u_m (both are equal for top-hat profiles). The second formula, proposed by Ricou and Spalding [43], takes into account the density difference between the jet and the ambient air by multiplying the right side of Eq. (8) by $(\rho/\rho_a)^{1/2}$. The use of $(\rho/\rho_a)^{1/2}$ to correct for dense jet effects has been often discussed in the literature. As recalled by Wheatley, this correction has been verified for single-phase gas jets at a normalized distance s/d_0 greater than 20 where the jet density was at most 5% higher than the ambient air. Since experimental observations of the behaviour of two-phase jets close to the outlet, suggesting that the initial jet angle is lower than the asymptotic value, are in contradiction with this correction, Wheatley concluded that this equation is not valid when the densities differ significantly from each other. We think that this correction, which is based on dimensional analysis, could be used for jet densities higher than $1.05\rho_a$, but its validity should be considered questionable close to the outlet since the complex flow development in this region, especially for two-phase flows, is not taken into account.

The cross-flow perpendicular to the jet axis is known to enhance the dilution of jets, which is attributed to the formation of a vortex-pair at the jet boundary (see, e.g., Coelho and Hunt [44]). This is modelled as a contribution proportional to the wind velocity component perpendicular to the jet:

$$E_2 = \alpha_2 \rho_a C |u_a \sin \theta|. \tag{9}$$

Some authors [16,34], following Ooms et al. [45], arbitrarily multiply E_2 by $\cos \theta$ to reduce its influence compared to that of E_1 at short distance from the outlet.

For the description of the atmospheric turbulence contribution, several approaches can be found. The first one, adopted by Muralidhar et al., has been proposed by Ooms et al. [45] who assumed that:

$$E_3 = \alpha_3 \rho_a C u', \tag{10}$$

where u' is a relevant atmospheric turbulent intensity. Pattison et al. use Eq. (10) with the friction velocity u_* instead of u'. Another approach consists of casting the well-known Gaussian model for passive atmospheric dispersion into the integral formulation. This leads to:

$$E_3 = \alpha_3 \pi \rho_a u_a \frac{\mathrm{d}}{\mathrm{d}x}(\sigma_y \sigma_z), \tag{11}$$

where σ_y and σ_z are the so-called Pasquill–Gifford horizontal and vertical dispersion coefficients, respectively. They depend on the atmospheric stability class and the distance from a suitably chosen virtual source. Following Havens et al. [46], Morud and

Selmer-Olsen multiply E_3 by $\cos \theta$ to limit its effect close to the source. It should be noted that the Pasquill–Gifford coefficients correspond to an averaging time of about 30 min, which leads to relatively low concentration and high air entrainment due to the meander of the cloud trajectory. Although noted by some authors (e.g. Ref. [32]), the possible inconsistency with shorter time scale phenomena (e.g. aerosol effects) has not yet been resolved. For ground-level clouds, a fourth contribution is sometimes used to take into account the suppression of turbulence due to heavy gas effects.

As can be seen from Table 2, the values of the empirical constants are quite different, reflecting a high uncertainty in modelling entrainment. Furthermore, the presence of the aerosol affects the turbulence structure of the jet. Indeed, compared to the turbulence intensity of the single-phase flow, the turbulence intensity of the gas phase in dispersed particulate flow, and therefore, air entrainment, is lower (resp. higher) when the particle diameter is below (resp. above) a critical value [47]. However, the degree of change depends on various parameters, e.g. it increases with the dispersed phase concentration, and is, until now, not predictable, although some attempts have been recently made [48]. This explains why this effect is disregarded in the models, or only taken implicitly into account through constant optimization. In the case of N_2/H_2O not-vaporizing two-phase jets associated with fine atomization, Seifert et al. [39] had to reduce the constant α_1 by approximately 20% when the exit gas quality was reduced to 0.4 to obtain a good fit to the data with their integral model predictions. MacGregor [49] measured the air entrainment in an industrial spray. Compared to single-phase results, he observed a more complex behavior and obtained an entrainment constant 30% higher. The presence of the aerosol phase, thus, remains a source of uncertainty in modelling air entrainment. Moreover, the sensitivity analysis performed by Pattison et al. with their model showed that an uncertainty of factor 4 on air entrainment prediction could completely change the trajectory of an upwardly inclined release.

3.2.4. Forces on the cloud

Models which do not include wind and gravity effects on the jet trajectory assume constant jet momentum so that $F_x = F_z = 0$ [8,14]. Other models contain a gravity term as a contribution of F_z. Most authors [9,16,22,32,34] also introduce an additional drag force F_D due to the cross-wind. This force is supposed to act in the direction perpendicular to the cloud axis. Its components in the x and z directions are therefore written as:

$$x - \text{direction: } F_{Dx} = C_D C \frac{1}{2} \rho_a (u_a \sin \theta)^2 \sin \theta, \tag{12}$$

$$z - \text{direction: } F_{Dz} = C_D C \frac{1}{2} \rho_a (u_a \sin \theta)^2 \cos \theta, \tag{13}$$

where C_D is a drag coefficient. A constant value of 0.3 is adopted by Woodward et al., Muralidhar et al. and Pattison et al. and a value of 0.2 is taken by Morud and Selmer-Olsen. For ground-level clouds, additional friction terms can be introduced [9] as well as gravitational forces in the x-direction [31,34]. According to Birch and Brown [50], the addition of a drag force may be useful to take into account the pressure gradient

perpendicular to the jet flow; however, the drag coefficient should be drastically lower than for the flow around a solid cylinder due to suction effects. The approach adopted in the above models is in contradiction with this recommendation. Moreover, according to Tickle [32], other forces on the jet may arise from deposition (rainout), curvatures of the jet and impact on the ground. They are, however, considered negligibly small.

3.2.5. Cloud thermodynamics

The enthalpy of the jet (mean or centreline value) is given by the two-phase mixture enthalpy balance equation (Eq. (5)). However, additional relationships are necessary to determine how the overall enthalpy change affects the jet composition and temperature. The jet is a mixture of the released material (liquid and/or vapour), dry air and, for all considered models but the one of Woodward et al., ambient humidity (liquid and/or vapour). Most often, the overall mixture enthalpy is expressed as a function of the enthalpies of the jet components by assuming that the mixture is in thermodynamic equilibrium. Gas and vapour are supposed to behave as an ideal gas. The partial pressures of the released material and the water are usually supposed to be given by their respective vapour pressure at the jet temperature (ideal mixture). However, in the case of ammonia, Wheatley took into account the non-ideality of the two-phase mixture behaviour. On the other hand, a thermodynamical non-equilibrium approach has been adopted by Woodward et al., Muralidhar et al. and Pattison et al. The mass and enthalpy equation (Eqs. (3) and (5)) are separately written for the liquid and gas phases. When ambient humidity condensation is considered, the liquid water is either included in the liquid phase leading to binary droplets [22] or added in the gas phase to form a fog [16]. Heat and mass transfer coefficients are introduced for transfers at the drop surface so that drops and gas or fog can adopt different temperatures.

Kukkonen et al. [29] and Nikmo et al. [30] checked the homogeneous equilibrium model predictions with those of a non-equilibrium approach (different velocities and temperatures for the droplets and the surrounding gas) in the case of two-phase ammonia cloud dispersion in dry and moist air. They concluded that the homogeneous equilibrium approximation seems to be adequate for droplet sizes lower than 100 μm. However, it is noted that this conclusion is only valid as far as the vaporization rate is concerned and may not apply to rainout. It may also not be valid for cases where entrainment is fast, as in the high momentum region of a jet. Indeed, measurements of Moodie and Ewan [40] suggest that thermodynamic equilibrium was not achieved in a distance of 200 diameters from the origin of a flashing jet of Refrigerant R-11. Moreover, Kukkonen et al. tested the effect of an introduction of ammonia/water interaction in the phase equilibrium. The assumption of non-ideal behaviour of the mixture lowered the volatility of the liquid phase, but exhibited no significant influence on the average temperature. It had, however, the effect of maintaining a low contaminant concentration much further downstream from the source. These authors also performed calculations with the assumption of zero and 100% ambient relative humidity. The difference in temperature could in some part of the dispersion reach 20 K. Similar calculations with Wheatley's model in the case of ammonia with zero and 100% ambient relative humidity have been also performed by Webber and Kukkonen [51]. The difference in the jet density and concentration for these extremes was less than 10%. However, the results were restricted

to the near-field where gravity effects were not considered significant. Furthermore, as shown by the sensitivity analysis performed by Pattison et al. [22] with their model, the high exothermic heat of mixing between water and hydrogen fluoride may cause the cloud to rise under humid conditions and to fall otherwise.

3.2.6. Rainout

As explained by Wheatley [3], provided that the drops are large enough, they are affected by gravity to a greater extent than the surrounding gas. The drops do not remain the same size during their motion but steadily evaporate as the surrounding vapour is diluted by air. From the spectrum of drop sizes formed initially, some drops may be large enough that they fall out of the jet rapidly with no appreciable vaporization, while others may be small enough that they evaporate before reaching the ground. The quantity of rainout is a very important item for dispersion calculations as shown, e.g. by the sensitivity analysis performed by Pattison et al. [22]. The description of this complex phenomenon is, however, circumvented by most modellers by assuming that the drops are sufficiently small to remain airborne until complete evaporation [31,32,34]. Wheatley [14] has devised a simple criterion for the absence of rainout, leaving aside the problem of what to do otherwise. From the maximum stable drop size in the initial section, the maximum gravitational settling velocity can be found from a force balance. By taking the drop axial velocity equal to the mean initial jet velocity (after the expansion zone), a bound for the initial drop trajectories can be defined. If it subtends a sufficiently small angle with the jet axis (taking it to be horizontal), this implies that rainout can be ignored. Ianello et al. [8] extended this approach by applying the above criterion to the whole spectrum of drop sizes. This enables the fraction of liquid which rains out to be calculated. A more sophisticated approach has been proposed by Woodward and Papadourakis [9]. The aerosol consists of single-sized spherical droplets. The local droplet diameter and trajectory is obtained by solving the balance equations on the drop for mass, energy and momentum in the vertical direction, simultaneously with the gas jet mean quantities. The horizontal drop velocity is set equal to the horizontal component of the local velocity in the jet, although in a previous version [52] a slip velocity was allowed for in the horizontal direction. Rainout occurs when the drop hits the ground. Muralidhar et al. [16] proposed another simple criterion. The liquid phase is supposed to be well mixed within the jet. Rainout is considered to occur when the jet centreline hits the ground (the liquid phase due to ambient humidity condensation is however supposed to remain airborne in the jet). Finally, Pattison et al. [22] calculate the rainout fraction with the relation empirically obtained by Schmidli [53] for instantaneous releases of Refrigerant R-114.

In accordance with the no-slip assumption made in the models, the drop inertia in the axial direction is not taken into account. Consequently, a relatively large drop which is not predicted to rainout according to Wheatley's approach, or which will fall out at a certain distance as predicted by Woodward's model, may eventually rainout further downstream. Also, as pointed out by Papadourakis et al. [54], the simple criteria of Wheatley, and Ianello et al. fail to rigorously account for the material evaporated from the droplets before rainout. Furthermore, Wheatley [3] recalled that impingement on a solid surface can cause deposition of a substantial fraction of the liquid component even

in the case where no rainout occurs without impingement. This contribution of rainout is however ignored in Wheatley's approach. On the contrary, this contribution is the only one taken into account by Muralidhar et al. [16], and Woodward and Papadourakis [9] consider both. However, any obstacle other than the ground seems not to have been considered.

Moreover, models which do not include a submodel for the droplet trajectory assume that the droplets are small enough to remain in suspension in the jet. In an earlier study, Woodward [55] used the results of correlations obtained in the field of pneumatic conveying of solids to argue that particles with the density of liquid chlorine would remain in suspension with particle sizes up to 1000 μm in case of a horizontal velocity of only 5 m/s. However, according to Morud and Selmer-Olsen [34], it is prudent to expect that only droplets of size less than 100 μm remain airborne. In the frame of our further investigations, we intend to propose a more rational way to justify this assumption by writing a more physical criterion for particle suspension. Following Peskin [56], the intensity of the turbulent field in the direction of gravity determines whether there is suspension. In particular, this component of turbulent energy must exceed the square of the free fall terminal velocity. Therefore, a practical criterion could be devised by comparing an estimate of the vertical turbulent intensity in the gas phase with the free fall velocity of the particle. It should be noted that, since the turbulent intensity decreases in the axial direction, a droplet which is initially in suspension could rainout further downstream. This criterion must therefore, be checked in each jet cross-section where the two phases are present.

Furthermore, in the most sophisticated approaches, the trajectory and evaporation of a typical drop is calculated. In the absence of sufficient liquid superheat for flashing atomization, a liquid core of length in the range of 200–500 orifice diameters will flow along with the droplets carrying the most part of liquid mass [28]. Its lower trajectory and evaporation rate may largely enhance the rainout fraction. Besides, the coalescence of droplets, which is sometimes mentioned as a possible important phenomenon, is rather unlikely to occur. Indeed, Faeth et al. [28] indicate that the liquid volume fraction in pressure-atomized sprays (which corresponds to liquid jets without flashing) is less than 0.1% outside the liquid core, which should be low enough for neglecting collision and coalescence [57]. Moreover, since in Woodward's approach a unique droplet size is considered, no rainout distribution on the ground can be obtained. This could however be easily modified by introducing an initial drop size distribution. Finally, the predictions of Schmidli's relation [53] adopted by Pattison et al. for the rainout fraction should be checked against rainout data for continuous release such as the ones obtained by Johnson and Diener [58]. This rainout fraction can have a strong influence on the trajectory and concentration of an upwardly inclined release, as shown by the sensitivity analysis performed by Pattison et al. [22].

3.2.7. Transition criteria

Generally, for some specific conditions, the model application range is exceeded or some model relationships must be modified. These conditions correspond to physical transitions for which criteria must be provided. First, a transition between elevated and ground-level clouds must be specified. This simply occurs when the lower boundary of

the jet reaches the ground. Moreover, for models which apply only in the region dominated by the initial jet momentum where gravity as well as atmospheric turbulence have no significant effect, transitions towards these regimes must be given. Citing Havens and Spicer [59], Ianello et al. [8] adopt the following criteria to determine when the dispersion is not dominated by the initial momentum any more:

$$\text{Passive dispersion important: } u_m/u_a \leq 0.8, \tag{14}$$

$$\text{Buoyancy effects important: } Ri = |\rho_m - \rho_a| gD/\rho_m u_m^2 \geq 0.1, \tag{15}$$

where D is the jet cross-section diameter and Ri the Richardson number of the jet which represents the ratio of jet buoyancy over jet inertia. Equivalent criteria are mentioned by the other authors when needed. During a parametric study performed by Webber and Kukkonen [51] and based on Wheatley's model for ammonia releases, they observed that, most often, gravity effects become important before the wind velocity is reached. However, Epstein et al. [31] showed from tests with their model on four field test experiments that the Richardson number never exceeds 0.1 in the whole dispersion range.

3.3. Multidimensional models

The two-phase multidimensional dispersion models that we consider subsequently are the one of Würtz et al. [4] and Bartzis [60], Garcia and Crespo [48], Vandroux-Koenig and Berthoud [23] and Pereira and Chen [24].

3.3.1. Würtz et al.'s model

This three-dimensional model includes the mixture mass, momentum and energy balance equations as well as the mass balance equation for the contaminant component [4,60]. The mixture is composed of the contaminant (liquid and/or gas) and the ambient gas (no humidity condensation is considered). Thermodynamical equilibrium is assumed, i.e. all the components share locally the same temperature and pressure. The two-phase mixture is supposed to behave ideally, i.e. Raoult's law is used for the calculation of the partial pressures. A single-phase turbulence model, based on the eddy diffusivity concept, is adopted and modified to take into account anisotropy effects. A vertical slip velocity is allowed for between the liquid and gas phase. Special attention was paid on the model's ability to handle complex terrain. In particular, liquid deposition on solid surfaces is taken into account. Remarks already made regarding the assumption of thermodynamic equilibrium in the integral models also apply here. The first validation tests performed by the authors [4] have shown the better performance of this model against a 1-D model when obstacles are present.

3.3.2. Garcia and Crespo's model

This three-dimensional model contains the mixture mass and momentum balance equations as well as the mass balance equation for the contaminant component [48]. The total enthalpy is taken proportional to the contaminant mass fraction. The treatment of the thermodynamics as well as the composition of the mixture are similar to Würtz et

al.'s model. The relative mean velocity between the phases is neglected. The classical $k - \epsilon$ model is used with an additional dissipation term due to the droplets.

3.3.3. Vandroux-Koenig and Berthoud's model

This model is devoted to the prediction of the near-field dispersion of liquefied propane [23]. It is a Eulerian–Eulerian two-fluid model which considers three components: propane (liquid and vapour), dry air and water (liquid and vapour). The condensed water is included in the gas phase to form a homogeneous fog mixture. Balance equations are written for the mass of each constituent, for the momentum of the gas mixture and of the propane droplets, and for the gas mixture energy. The temperature of the propane droplets is supposed to be uniform, equal to the saturation temperature at atmospheric pressure, so that no energy balance equation is needed for the liquid phase. To close the system of equations, a single-phase turbulence model based on the Prandtl's mixing length theory is introduced for the gas phase. For interfacial transfers, a constant droplet diameter is assumed throughout the calculation. The momentum and heat interfacial transfer terms are calculated from a drag and a heat transfer coefficient, respectively, for rigid spheres. The mass transfer is modelled by assuming that the heat transferred from the gas phase to the droplets completely contributes to vapour production.

According to the authors, the propane droplets are predicted to persist much further downstream than experimentally observed. Several possible causes were investigated for this underestimation of droplet evaporation. Neither the assumption of a constant diameter nor the fact that no initial radial velocity was taken into account could explain this underevaluation. On the other hand, the assumption of a uniform temperature in the droplet or the inadequacy of the turbulence model (the droplets may in reality disperse more than the gas phase) have been proposed as possible explanations. One important assumption which could strongly hamper evaporation and which was not yet discussed, is to take the droplet temperature equal to the saturation temperature at ambient pressure instead of the one corresponding to the vapour partial pressure at the surface (lower due to the dilution of the contaminant vapour). This assumption contradicts the experimental observation that liquid temperature can decrease below the normal boiling point (e.g. Ref. [61]). A more complex model which takes into account the mass diffusion around the droplet such as the one adopted by Woodward and Papadourakis [9] and Woodward et al. [15] should be introduced. More parametric studies as well as the comparison of the prediction with the results of controlled laboratory experiments adapted to the validation of the uncertain aspects of the model are required to solve these inconsistencies.

3.3.4. Pereira and Chen's model

This Eulerian–Lagrangian model [24] is also devoted to the near-field dispersion of liquefied propane; the single-phase version developed for the far-field dispersion is not considered here. It is constituted of a Eulerian description of the mixture phase composed of air and propane vapour (no humidity is taken into account) having the same velocity and temperature but different volume fractions, and a Lagrangian modelling of the droplet phase which is composed of various droplet-size groups having

their own initial characteristics (velocity, temperature, diameter, ...). In the gas phase, the $k - \epsilon$ model is adopted. The effect of the dispersed phase on the gas phase is limited to the mass, momentum and enthalpy transport due to the phase–change process. For each of the two size classes of droplets, the equation of motion is written. The interfacial force is determined by using a drag coefficient valid for solid spheres and with the relative velocity evaluated from the mean local gas velocity. The heat and mass transfer is calculated with a heat transfer coefficient for a rigid sphere and by assuming that the heat transferred from the gas phase to the droplet contributes completely to the evaporation. The surface temperature of the propane droplets is supposed to be equal to the saturation temperature at atmospheric pressure.

According to Berlemont et al. [62], the Lagrangian approach has the advantage to account for the instantaneous flow properties encountered by the particles. A second cited advantage of the Eulerian–Lagrangian approach is the possibility to readily handle the evolution of a distribution of particle diameters, which remains difficult to predict in a Eulerian–Eulerian scheme. However, transient situations are more easily solved by a Eulerian–Eulerian approach. This seems to favour the choice of Lagrangian models for the description of the continuous releases considered here. The first advantage is, however, not used by Pereira and Chen since only the mean local gas characteristics are taken into account in the droplet equations. Moreover, the comparison with Vandroux-Koenig and Berthoud's model reported by Pereira and Chen [24] showed no major discrepancies so that the droplet evaporation must also be underevaluated. As for Vandroux-Koenig and Berthoud's model, this underevaluation may be attributed to the inadequacy of the droplet evaporation model.

4. Experimental data and model validation

The parameters of field experiments [58,61,63–74] as well as laboratory experiments [16,25,39,40,75,76] for continuous two-phase jet dispersion are given in Tables 3 and 4, respectively. The data generally include source term characteristics (e.g. diameter and height of the release, mass flow rate, properties of the exiting fluids, ...) and ambient conditions (e.g. wind speed, atmospheric stability, relative humidity, ...) which can be used as input parameters for the calculations. They also provide a part of the following information which can be used for model validation: (1) contaminant concentration at a fixed elevation as a function of the distance from the outlet, (2) contaminant concentration contours in a cross-wind plane, (3) temperature at a fixed elevation in the jet as a function of the distance from the outlet, (4) temperature contours in a cross-wind plane, (5) temperature at the ground surface as a function of the distance from the outlet, (6) velocity contours in a jet cross-section, (7) presence or absence of a pool on the ground, (8) quantity of rainout, (9) visibility range of the cloud (due to water or contaminant aerosol), and (10) droplet size. For a more detailed description of the experiments, the reader is referred to the original reports or to other reviews, e.g. [14,34,77]. From the tables, it can be seen that a wide enough range of fluids was studied but only a few fully instrumented experiments have been performed, especially regarding local velocity and drop size. Also, rainout experiments have appeared recently, indicating a growing interest in this phenomenon.

Table 3
Fluids and properties measured in field test experiments

Test	Fluids	Concentration	Temperature	Velocity	Rainout	Visibility	Drop size
Resplandy	NH_3	−	−	−	+	+	−
Nyren and Winter (Landskrona)	NH_3	−	−	−	+	+	−
Goldwire et al. (Desert Tortoise)	NH_3	+	+	−	+	+	−
Nyren and Winter (Boliden)	SO_2	−	−	−	+	+	−
Blewitt et al. (Goldfish)	HF	+	+	−	+	+	−
Pfenning et al.	NH_3, propane	−	−	−	+	+	−
Heinrich et al.	propane	+	−	−	+	+	−
Lantzy et al.	methylamine	−	−	−	+	+	−
Johnson et al.	H_2O, CFC-11, CL_2, methylamine, cyclohexane	−	−	−	+	−	−
Schumann et al.	propane	+	+	+	+	+	+
Schatz et al.	HF/additives	−	−	−	+	−	−
Nielsen and Ott (Fladis)	NH_3	+	+	−	+	−	−

Since the main goal of a dispersion model is to calculate the contaminant concentration in space and time, item (1) and (2) could be considered as permitting an overall validation of the models, whereas the other quantities are more useful for validation of submodels. However, it should be noted that, partly depending on each model formulation, the data may not all be adequate for model validation. Also, due to their scale and their safety requirements, field experiments are difficult to perform, which limit their number and their completeness for model validation. In particular, uncertainties in the knowledge of the ambient conditions limit the appropriateness of the field experiment for testing models, as has been already stressed by several authors [34]. Besides, the literature cited here is more particularly related to two-phase jet dispersion. Experimen-

Table 4
Fluids and properties measured in laboratory experiments

Test	Fluids	Concentration	Temperature	Velocity	Rainout	Visualization	Drop size
Seifert et al.	H_2O/N_2, CO_2	+	−	+	−	+	−
Moodie and Ewan	R-11	+	+	+	−	+	+
Hague and Pepe	HF	−	−	−	+	−	−
Muralidhar et al.	HF/additives	−	−	−	+	−	−
Hervieu and Veneau	propane	−	−	+	−	+	+
Allen	propane	−	+	+	−	−	+

tal data for other types of dispersion (e.g. pure gas), from other fields (e.g. atomization) or of a more fundamental nature (e.g. turbulence in two-phase flow) should also be used for validation of submodels. In particular, a decoupled optimization procedure was adopted by Woodward et al. [15] to tune their model, making use of sets of data adapted to each part of the model; an overall validation of the model on a data set not used for model optimization was, however, not shown. In general, the validation presented by the authors of each model always comprises comparison with a few selected experiments if any, which does not allow a firm judgement to be made on the model quality. Independent model evaluation, such as the one performed by Hanna et al. [77], is therefore, clearly needed.

5. Conclusion

This review has been focused on the comparative description of two-phase jet dispersion models, with special attention to elevated and continuous conditions. A description of available data for two-phase jet dispersion was also given. Both integral and multidimensional models were considered.

Most often, the integral approach has been adopted because of its good compromise between model detail and computing time/cost, which is well adapted to hazard assessment. In integral models, entrainment modelling remains an important issue, as reflected by the differences between adopted formulations. Regarding two-phase flow phenomena, the homogeneous equilibrium approximation is often used. The range where this is justified has, however, not been defined in the case of high momentum jets. When this approximation is, at least partially relaxed, the prediction of the initial drop size, drop trajectory and possibly evaporation is required. The corresponding submodels show however a rather high degree of simplification and uncertainty. Some propositions for their verification and improvement have been given. They include the comparison of the submodels' prediction to recent experimental data, the extension of models to non-flashing two-phase releases and a rational criterion for droplet suspension in a jet.

Multidimensional models have been shown to be valuable for dispersion calculation in complex environment. Although the required closure relations are generally different compared to that in the integral models (turbulence instead of entrainment models), the ones concerning the droplet phase are rather similar and present the same kind of uncertainty.

Generally speaking, the models are insufficiently validated. To be able to give a firm judgement of their quality, an independent evaluation is clearly needed. For this purpose, additional detailed two-phase jet experiments should be performed.

Acknowledgements

References

[1] R.E. Britter, Atmospheric dispersion of dense gases, Ann. Rev. Fluid Mech. 21 (1989) 317–344.

[2] H.K. Fauske, M. Epstein, Hazardous vapor clouds: release type, aerosol formation and mitigation, in: Proc. 6th Int. Symp. Loss Prevention and Safety Promotion in the Process Industries, Vol. II, 1989, pp. 69/1–69/15.

[3] C.J. Wheatley, Factors affecting cloud formation from releases of liquefied gases, in: Proc. IChemE Symposium on Refinement of Estimates of the Consequences of Heavy Toxic Vapour Releases, UMIST, 1986.

[4] J. Würtz, J. Bartzis, A. Venetsanos, S. Andronopoulos, J. Statharas, R. Nijsing, A dense vapour dispersion code package for applications in the chemical and process industry, J. Hazard. Mater. 46 (1996) 273–284.

[5] R.E. Britter, The modelling of a pseudo-source for complex releases, FM89/2, Cambridge Environmental Research Consultants, 1994.

[6] R.E. Britter, A further note on modelling flashing releases, FM89/3, Cambridge Environmental Research Consultants, 1995.

[7] J.L. Woodward, Expansion zone modeling of two-phase and gas discharges, DIERS Minutes 12, 1992.

[8] V. Ianello, P.H. Rothe, G.B. Wallis, R. Diener, S. Schreiber, Aerosol research program: improved source term definition for modeling the ambient impact of accidental release of hazardous liquids, in: Proc. 6th Int. Symp. Loss Prevention and Safety Promotion in the Process Industries, 1989, pp. 58/1–58/30.

[9] J.L. Woodward, A. Papadourakis, Modeling of droplet size, evaporation, and rainout in a dispersing aerosol jet, in: Proc. Int. Conf. and Exhibition on Safety, Health, and Loss Prevention in the Oil, Chemical, and Process Industries, Singapore, 1993, pp. 553–569.

[10] J.L. Woodward, A. Papadourakis, Reassessment and reevaluation of rainout and drop size correlation for an aerosol jet, J. Hazard. Mater. 44 (1995) 209–230.

[11] R. Brown, J.L. York, Sprays formed by flashing liquid jets, AIChE J. 8 (2) (1962) 149–153.

[12] D.M. Bushnell, P.B. Gooderum, Atomization of superheated water jets at low ambient pressures, J. Spacecraft Rockets 5 (2) (1968) 231–232.

[13] Y. Kitamura, H. Morimitsu, T. Takahashi, Critical superheat for flashing of superheated liquid jets, Ind. Eng. Chem. Fundam. 25 (1986) 206–211.

[14] C.J. Wheatley, Discharge of ammonia to moist atmospheres—survey of experimental data and model for estimating initial conditions for dispersion calculations, SRD R410, UKAEA, 1987.

[15] J.L. Woodward, J. Cook, A. Papadourakis, Modeling and validation of a dispersing aerosol jet, J. Hazard. Mater. 44 (1995) 185–207.

[16] R. Muralidhar, G.R. Jersey, F.J. Krambeck, S. Sundaresan, A two-phase release model for quantifying risk reduction for modified HF alkylation catalysts, J. Hazard. Mater. 44 (1995) 141–183.

[17] N.J. Kolev, Fragmentation and coalescence dynamics in multiphase flows, Exp. Thermal Fluid Sci. 6 (1993) 211–251.

[18] R. Clift, J.R. Grace, M.E. Weber, Bubbles, Drops and Particles, Academic Press, New York, 1978.

[19] A.H. Lefebvre, Properties of sprays, Part. Part. Syst. Charact. 6 (1989) 176–186.

[20] M.M. Elkotb, Fuel atomization for spray modelling, Prog. Energy Combust. Sci. 8 (1) (1982) 61–91.

[21] K. Forster, N. Zuber, Dynamics of vapor bubbles and boiling heat transfer, AIChE J. 1 (1955) 531–535.

[22] M.J. Pattison, R. Martini, S. Banerjee, G.F. Hewitt, Modelling of dispersion of two-phase releases, submitted to Process Safety and Environment Protection.

[23] S. Vandroux-Koenig, G. Berthoud, Modelling of a two-phase momentum jet close to the breach, in the containment vessel of a liquefied gas, J. Loss Prev. Process Ind. 10 (1) (1997) 17–29.

[24] J.C.F. Pereira, X.-Q. Chen, Numerical calculation of unsteady heavy gas dispersion, J. Hazard. Mater. 46 (1996) 253–272.

[25] E. Hervieu, T. Veneau, Experimental determination of the droplet size and velocity distributions at the exit of the bottom discharge pipe of a liquefied propane storage tank during a sudden blowdown, J. Loss Prev. Process Ind. 9 (6) (1996) 413–425.

[26] H. Lemonnier, E.S. Camelo-Cavalcanti, Droplet size and velocity at the exit of a nozzle with two-component near-critical and critical flow, in: ANS Proceedings National Heat Transfer Conference, Vol. 7, 1993, pp. 93–100.

[27] R.J. Bettis, P.F. Nolan, K. Moodie, Two-phase flashing releases following rapid depressurisation due to vessel failure, in: Hazards from Pressure: Exothermic Reactions, Unstable Substances, Pressure Relief and Accidental Discharge, IChemE Symposium Series No. 102, 1987, pp. 247–263.

[28] G.M. Faeth, L.-P. Hsiang, P.-K. Wu, Structure and breakup properties of sprays, Int. J. Multiphase Flow 21 (1995) 99–127, Suppl.

[29] J. Kukkonen, M. Kulmala, J. Nikmo, T. Vesala, D.M. Webber, T. Wren, Aerosol cloud dispersion and the suitability of the homogeneous equilibrium approximation, AEA/CS/HSE R1003/R, AEA Technology, 1993.

[30] J. Nikmo, J. Kukkonen, T. Vesala, M. Kulmala, A model for mass and heat transfer in an aerosol cloud, J. Hazard. Mater. 38 (1994) 293–311.

[31] M. Epstein, H.K. Fauske, G.M. Hauser, A model of the dilution of a forced two-phase chemical plume in a horizontal wind, J. Loss Prev. Process Ind. 3 (1990) 280–290.

[32] G.A. Tickle, An integral model for an elevated two-phase jet in a cross-flow, in: Heat Transfer, AIChE Symposium Series No. 288, Vol. 88, 1992, pp. 350–356.

[33] G.A. Tickle, S.J. Jones, D. Martin, S.A. Ramsdale, D.M. Webber, Development and validation of integral models of two-phase jets, AEAT/1389, AEA Technology, 1997.

[34] S. Morud, S. Selmer-Olsen, Modelling dense gas dispersion of propane (LPG) from high momentum release sources forming aerosols, Final report, CEC Program: Major Technological Hazards, 1994.

[35] S. Banerjee, R. Martini, M.J. Pattison, Cloud: a vapour-aerosol dispersion model accounting for plume 3D motion and heat and mass transfer between phases, J. Hazard. Mater. 46 (1996) 231–240.

[36] R.P. Cleaver, P.D. Edwards, Comparison of an integral model for predicting the dispersion of a turbulent jet in a cross-flow with experimental data, J. Loss Prev. Process Ind. 3 (1990) 91–96.

[37] G.A. Davidson, Gaussian versus top-hat profile assumptions in integral plume models, Atmos. Environ. 20 (3) (1986) 471–478.

[38] J. Popper, N. Abuaf, G. Hetsroni, Velocity measurements in a two-phase turbulent jet, Int. J. Multiphase Flow 1 (1974) 715–726.

[39] H. Seifert, H. Giesbrecht, W. Leuckel, Dispersion of heavy gases and single- and two-phase vapours escaping from vertical outlets, Ger. Chem. Eng. 7 (1984) 126–137.

[40] K. Moodie, B.C.R. Ewan, Jets discharging to atmosphere, J. Loss Prev. Process Ind. 3 (1990) 68–76.

[41] G.A. Tickle, D.M. Webber, Part II: Modelling jets in an ambient flow, Report SRD/CEC/22939/01, AEA Technology, 1992.

[42] B.R. Morton, G.I. Taylor, J.S. Turner, Turbulent gravitational convection from maintained and instantaneous sources, Proc. R. Soc. 234 A (1956) 1–22.

[43] F.P. Ricou, D.B. Spalding, Measurements of entrainment by axisymmetrical turbulent jets, J. Fluid Mech. 11 (1961) 21–32.

[44] S.L.V. Coelho, J.C.R. Hunt, The dynamics of the near field of strong jets in cross-flows, J. Fluid Mech. 200 (1989) 95–120.

[45] G. Ooms, A.P. Mathieu, F. Zelis, The plume path of vent gases heavier than air, in: Proc. 1st Int. Symp. on Loss Prevention and Safety Promotion in the Process Industries, 1974, pp. 211–219.

[46] J.A. Havens, T.O. Spicer, D.W. Guinnup, Extension of the DEGADIS atmospheric dispersion model for elevated jet releases, in: Proc. 6th Int. Symp. Loss Prevention and Safety Promotion in the Process Industries, 1989, pp. 72/1–72/30.

[47] R.A. Gore, C.T. Crowe, Effect of particle size on modulating turbulent intensity, Int. J. Multiphase Flow 15 (2) (1989) 279–285.

[48] J. Garcia, A. Crespo, A model of turbulent two-phase flashing jets, 1997 ASME Fluids Engineering Division Summer Meeting, 1997, pp. 1–6.

[49] S.A. MacGregor, Air entrainment in spray jets, Int. J. Heat Fluid Flow 12 (3) (1991) 279–283.

[50] A.D. Birch, D.R. Brown, The use of integral models for predicting jet flows, in: C.A. Cox (Ed.), Mathematics in Major Accident Risk Accident, 1989.

[51] D.M. Webber, J.S. Kukkonen, Modelling two-phase jets for hazard analysis, J. Hazard. Mater. 23 (1990) 167–182.

[52] J.L. Woodward, A. Papadourakis, Modeling of droplet entrainment and evaporation in a dispersing aerosol jet, in: Proc. Int. Conf. and Workshop on Modeling and Mitigating the Consequences of Accidental Releases of Hazardous Materials, New Orleans, AIChE, 1991, pp. 147–168.

[53] J. Schmidli, The initial phase of sudden releases of superheated liquid, PhD Thesis, Swiss Federal Institute of Technology, Zürich, 1993.

[54] A. Papadourakis, H.S. Caram, C.L. Barner, Upper and lower bounds of droplet evaporation in two-phase jets, J. Loss Prev. Process Ind. 4 (1991) 93–101.

[55] J.L. Woodward, Dispersion modelling of an elevated high momentum release forming aerosols, J. Loss Prev. Process Ind. 2 (1989) 22–32.

[56] R.L. Peskin, Turbulent fluid–particle interaction, in: G. Hetsroni (Ed.), Handbook of Multiphase Systems, Hemisphere, 1982.

[57] Y. Hardalupas, A.M.K.P. Taylor, J.H. Whitelaw, Velocity and particle-flux characteristics of turbulent particle-laden jets, Proc. R. Soc. London A 426 (1989) 31–78.

[58] D.W. Johnson, R. Diener, Prediction of aerosol formation from the release of pressurized, superheated liquids to the atmosphere, in: Hazards XI, 11th Symposium on New Directions in Process Safety, IChemE Symposium Series No. 124, 1991, pp. 87–104.

[59] J.A. Havens, T.O. Spicer, A dispersion model for elevated dense gas jet chemical releases, Final report, Environmental Protection Agency, 1988.

[60] J.G. Bartzis, ADREA-HF: a three-dimensional finite volume code for vapour cloud dispersion in complex terrain, EUR 13580 EN, 1991.

[61] H.C. Goldwire Jr., T.G. McRae, G.W. Johnson, D.L. Hipple, R.P. Koopman, J.W. McClure, L.K. Morris, R.T. Cederwall, Desert Tortoise series data report: 1983 pressurized ammonia spills, UCID-20562, LLNL, Livermore, CA, USA, 1985.

[62] A. Berlemont, M.S. Grancher, G. Gouesbet, Heat and mass transfer coupling between vaporizing droplets and turbulence using a Lagrangian approach, Int. J. Heat Mass Transfer 38 (16) (1995) 3023–3034.

[63] A. Resplandy, Etude expérimentale des propriétés de l'ammoniac conditionnant les mesures à prendre pour la sécurité du voisinage des stockages industriels, Chim. Indus. Génie Chim. 102 (1969) 691–702.

[64] K. Nyren, S. Winter, Two-phase discharge of liquefied gases through pipes. Field experiments with ammonia and theoretical model, in: 4th Int. Symp. on Loss Prevention and Safety Promotion in the Process Industries, IChemE Symp. Series No. 80, 1983.

[65] K. Nyren, S. Winter, Discharge of condensed sulfur dioxide: a field test study of the source behaviour with different release geometries, J. Hazard. Mater. 14 (1987) 365–386.

[66] D.N. Blewitt, J.F. Yohn, R.P. Koopman, T.C. Brown, Conduct of anhydrous hydrofluoric acid spill experiments, in: Proc. Int. Conf. Vapor Cloud Modeling, 1987, pp. 1–38.

[67] B.D. Pfenning, S.B. Millsap, D.W. Johnson, Comparison of turbulent jet model predictions with small-scale pressurized releases of ammonia and propane, in: Proc. Int. Conf. on Vapor Cloud Modeling, 1987.

[68] M. Heinrich, E. Gerold, P. Wietfeldt, Large scale propane release experiments over land at different atmospheric stability classes, J. Hazard. Mater. 20 (1988) 287–301.

[69] M. Heinrich, E. Gerold, P. Wietfeldt, Large scale propane release experiments over land at different atmospheric stability classes, J. Hazard. Mater. 22 (1989) 407–413.

[70] R.J. Lantzy, R.D. Myers, D.B. Pfenning, S.B. Millsap, Atmospheric release tests of monomethylamine, J. Loss Prev. Process Ind. 3 (1990) 77–81.

[71] S. Schumann, W. Haas, H. Schmittberger, I. Wirkner-Bott, M. Stock, Large scale experiments on two-phase jet releases, Final report, CEC Program: Major Technological Hazards, 1992.

[72] S. Schumann, An experimental and modelling study of two-phase flashing jets, Final report, CEC: Environment Programme, 1997.

[73] K.W. Schatz, G.R. Jersey, M.K. Chalam, D.W. Johnson, Apparatus for field testing of HF releases, AIChE Summer National Meeting, Seattle, 1993.

[74] M. Nielsen, S. Ott, Fladis field experiments—final report, Risoe-R-898(EN), Risoe National Laboratory, Roskilde, Denmark, 1996.

[75] W.J. Hague, W. Pepe, Flow chamber simulations of aerosol formation and liquid jet breakup for pressurized releases of hydrogen fluoride, Plant/Operations Prog. 9 (2) (1990) 125–130.

[76] J.T. Allen, Laser-based droplet size measurements in two-phase flashing propane jets, HSL Report IR/L/FR/96/6, HSL, Harpur Hill, Buxton, UK, 1996.

[77] S.R. Hanna, J.C. Chang, D.G. Strimaitis, Hazardous gas model evaluation with field observations, Atmos. Environ. 27A (15) (1993) 2265–2285.